Materials and Design 35 (2012) 175–183

Contents lists available at SciVerse ScienceDirect

Materials and Design

journal homepage: www.elsevier.com/locate/matdes

Microstructures and fatigue properties of friction stir lap welds in aluminum alloy AA6061-T6

Xiaodong Xu [a], Xinqi Yang [a,*], Guang Zhou [a], Jianhua Tong [b]

[a] Tianjin Key Laboratory of Advanced Joining Technology, School of Materials Science and Engineering, Tianjin University, Tianjin 300072, China
[b] China FSW Center, Beijing FSW Technology Limited Company, Beijing 100024, China

ARTICLE INFO

Article history:
Received 4 July 2011
Accepted 28 September 2011
Available online 5 October 2011

Keywords:
A. Non-ferrous metals and alloys
D. Welding
E. Fatigue

ABSTRACT

Microstructural features and fatigue properties of friction stir lap-welded joints for AA6061-T6 alloy are investigated and the influences of single pass welding (SPW) or double pass welding (DPW), hooking defects and fatigue stress ratio on the fatigue properties are analyzed. It is found that the fatigue strengths of FSW lap-welded joints are obviously lower than that of the fusion lap-welded joints of IIW FAT22 and only approximately correspond and close to the IIW FAT12 design curve. The higher fatigue stress ratio R will lead to the decrease of the fatigue strength of lap-welded joints. The existence of hooking defects is the key factor to reduce the fatigue strengths. Fatigue cracks always initiate at the tip of hooking defect in the RS of SPW and AS of DPW joints respectively. The severity of hooking defects and the quality of lap-welds could not be improved by the DPW process as compared with the SPW process. The fatigue strength $\Delta\sigma_m$ and $\Delta\sigma_k$ ($R = 0.1$) of DPW joints will be 21.26% and 17.88% lower than that of SPW joints respectively. The fracture of lap-welded joints exhibits multiple crack initiations from the tips of the hooking locations, and the crack propagation shows some brittle fracture and is mainly characterized by the fatigue striations. The locations of crack initiation and the amount of secondary cracks in DPW joints are more than that of in the SPW joints which leading to the lower fatigue properties. The ductile fracture mode is obviously shown in the final fracture zone with deep-hole type dimples in the SPW joints but shallow-hole type dimples in the DPW joints.

1. Introduction

Friction stir welding (FSW) is an advanced solid-state joining process that was invented by The Welding Institute (TWI) of United Kingdom in 1991 [1], and it is mainly suitable for the joining of aluminum alloys that are always difficult to be welded by the traditional fusion methods without solidifying cracks, porosity or distortion, etc. Currently FSW technology has been highly developed and widely used in many structural manufacturing fields such as the aerospace and airplane, ship-construction, high-speed train and automotive industries for high-performance structural demanding applications [2,3]. The aluminum alloys of 6xxx-series, containing magnesium and silicon as major alloying elements, have attractive combinations of properties such as high strength, formability, fatigue resistance and relatively low cost [4,5] and are one of the widely used aluminum alloys in the above mentioned industrial fields. The investigations on the friction stir welded 6xxx-series aluminum alloy technologies are really necessary and important for the industrial application of FSW.

Up to now many researches on the FSW for aluminum alloys butt-welded joints have been reported such as the features of stirring zone microstructures, the distributions of micro-hardness, the formations of various defects and bonding strength have all been discussed in depth [6,7]. In recent years, much attention has been focused on the FSW lap-welded joints in order to verify their bearing capabilities to replace riveted joints in aircraft structures. Actually, airplane panels, wing frames and floor decks are often strengthened with stringers and profiles are always welded to the outer skin with lap-welded joints [8,9]. In addition, automotive engine frames, wheel rims, car back supports and hermetically closed boxes such as cooling elements and heat exchangers all inevitably involve lap-welded joints [10].

It has been shown that concerning static strength, FSW lap-welded joints can be comparable with resistance spot welded and riveted joints. But as for fatigue performances it was obviously lower than that of butt-welded joints [11–13]. The peculiarity of FSW lap-welded joints with respect to butt ones is that two crack-like weak-bonded regions are inevitably present at the ends of lap interfaces (the hooking defects). These should induce the severely stress concentrations and the net reduction of the cross section of sheets and lower the strength of the joint especially in fatigue [14]. How to eliminate or reduce the stress concentrations

* Corresponding author. Tel./fax: +86 22 2740 7022.
E-mail address: xqyang@tju.edu.cn (X.Q. Yang).

0261-3069/$ - see front matter © 2011 Elsevier Ltd. All rights reserved.
doi:10.1016/j.matdes.2011.09.064

and understand the fatigue properties of FSW lap-welded joints should be the urgently solved problems for the industrial applications. Recently, some related research institutes are working on improving the fatigue properties of lap-welded joints. Much efforts have been made for developing specific shapes of tools (such as Flared-Triflute™, Skew-Stir™, Re-Stir™ and Trivex™) for FSW lap-welded joints [8,15], which could allow to promote the material plastic flow around tool pin to minimize hooking degree of the sheet interface adjacent to the weld nugget. Besides the broader tool shoulder with a concave end of tool pin design could provide the better fatigue performance due to the increased contact area and the improved flow path provided by the hollowed out end of the pin [10].

It should be emphasized that the fatigue performances are known to be one of the crucial assessment qualities for the structural materials bearing the dynamical loading, and because of the effects of random and statistical factors on fatigue behaviors it is very important to accumulate the fatigue testing results under various conditions. However, currently the general fatigue assessment specification of FSW welded joints and components have not been established. Especially for FSW lap-welded joints the fatigue behaviors for aluminum alloys are really seldom in publications. Some influence factors such as the pass number that is the double pass welded (DPW) or single pass welded (SPW), the hooking defect and fatigue stress ratio (R) for FSW lap-welded joints on the fatigue properties are unclear and unspecific. This work concentrated on the understanding of microstructural features and fatigue properties of AA6061-T6 FSW lap-welded joints. Fatigue specimens made by SPW and DPW lap joints were tested under load control with different fatigue stress ratio (R) to do contrast analysis and the effects of hooking defects on the fatigue properties of FSW lap-welded joints were discussed. The fatigue life and fatigue strength characteristic values were calculated in accordance with the IIW recommendations [16] and the fracture surfaces were observed to examine the fatigue fracture features of FSW lap-welded joints.

2. Experimental procedures

The base materials used for the experiment were AA6061-T6 plates with thickness 5 mm, and the fatigue specimens were made by the friction stir single pass welded (SPW) and double pass welded lap-plate components. The chemical compositions in mass% of base metals (BMs) AA6061-T6 is 0.92Mg, 0.68Si, 0.43Cu, 0.33Fe, 0.013Mn, 0.01Ti, 0.01Zn, Al balance. The mechanical properties of AA6061-T6 are shown in Table 1. All of the welds were produced with the rotational speed (ω) of 1400 rpm, the traveling speed (v) of 400 mm/min, the tilt angle of 2.5° and the rotation direction of counterclockwise. Other detailed welding parameters are proprietary to the China FSW Center Beijing FSW Technology Limited Company. The welding processes of SPW and DPW were illustrated in Fig. 1, and the second pass weld of DPW process was done at the same position of the first pass weld by using the same welding parameters. The aim of performing DPW process was intended to evaluate whether the second pass weld could reduce the hooking degree and improve the lap-weld quality. After welding, all the welds were examined by using X-ray radiographs non-destructive method and no flaws were detected. Then the fatigue specimens were machined from the flaw-free lap-welded plate components.

Table 1
Mechanical properties of AA6061-T6.

Material	Yield stress $\sigma_{0.2}$ (MPa)	Tensile stress σ_b (MPa)	Elongation (%)
6061	280	295	12

Because of no fatigue testing methods for FSW lap-welded joints, the standard of JIS Z 3138 [17] method of fatigue testing for spot welded joints was referred to determine the sizes and shapes of FSW lap-welded specimens as shown in Fig. 2 and the statistical evaluation of fatigue test data suggested by IIW recommendations was used to deal with the S–N curves of FSW lap-welded joints.

The fatigue experiments were carried out using a high frequency fatigue testing machine with a capacity of 100 kN loads. Before fatigue testing, all the lateral edges of fatigue specimens were polished in order to avoid the influence of local surface stress concentration. A sinusoidal load–time function was used with the fatigue stress ratio R ($=\sigma_{min}/\sigma_{max}$) set to 0.1 and 0.5 for SPW joints, 0.1 and 0.3 for DPW joints, respectively. There were thirty-two fatigue specimens were performed in testing study, in which 10 specimens were SPW joints for $R = 0.1$, nine were SPW joints for $R = 0.5$, seven were DPW joints for $R = 0.1$ and six were DPW joints for $R = 0.3$, respectively. The oscillation frequency of fatigue testing machine was shown between 90 and 95 Hz in laboratory atmosphere.

In order to analyze microstructural features, the specimens were crossly cut perpendicular to the FSW direction, which were grinded and polished, then etched by Keller's reagent with the following composition: 2 ml hydrofluoric acid, 3 ml hydrochloric acid, 5 ml nitric acid and 95 ml water, washed in water, dried with ethanol and finally observed by the optical microscope OLYMPUS-GX51. The fatigue fracture surface was examined and observed by using the scanning electron microscopy (SEM) of Hatchi S-4800.

3. Results and discussion

3.1. Macro and microstructures of lap-welded joints

Fig. 3a and b shows typical cross section macrostructures of the AA6061-T6 friction stir lap-welded joints under two conditions. The SPW joint has an elliptical nugget zone while the DPW joint has a basin-shaped nugget zone. Both FSW lap-welded joints consist of four zones: non-affected base metal (BM), nugget zone (NZ) around the weld center line, thermal mechanical affected zone (TMAZ) on both sides of the NZ and heat affected zone (HAZ) that is surrounding the TMAZ [18]. According to the direction relationships between ω and v, two sides can be defined: the same is the advancing side (AS) and the opposite is the retreating side (RS).

It was clearly observed the original faying surfaces between the top and bottom sheets in lap-welded joints. One notable feature was that these interfaces experienced deformations and offset from the original straight direction in TMAZ (Fig. 3a and b). This distorted interface is usually termed as the hooking defect in the friction stir lap-welded joints [19]. These special defects are produced by the characteristics of friction stir lap-welding technology processes. Unlike the FSW butt-welding processes that the bonding surfaces are parallel to the axial line of stirring pin, the bonding interfaces of lap-welding processes are vertical to that of stirring pin. In order to stir and mix the lap-interfaces sufficiently, the stirred thermal-plastic base metal around the pin not only performs axial flow and mix, but also has up and down flow and mix along the thickness direction. Therefore the tips of lap-interfaces around the nugget zone will be offset from the original lap-interfaces and form the "hooking defects". As the consequence of the tips of hooking interface extending into top sheet, the "effective sheet thickness" (EST) of lap-welded joints are obviously reduced. The EST is defined as the minimum sheet thickness determined by measuring the smallest distance between any un-bonded interface and the top surface of the upper sheet or the bottom surface of the lower sheet. These phenomena should have apparent influences on the bearing-load of FSW lap-welded joints. It is examined that the

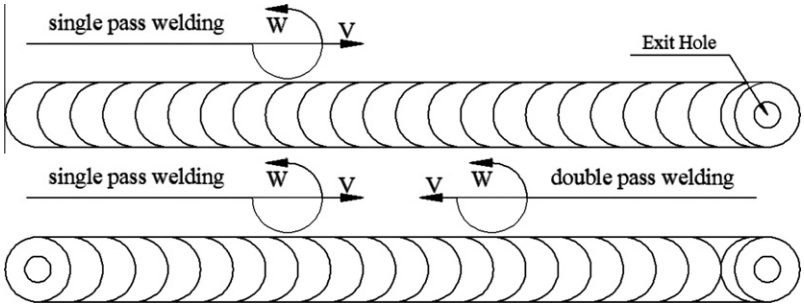

Fig. 1. Schematic diagram of SPW and DPW.

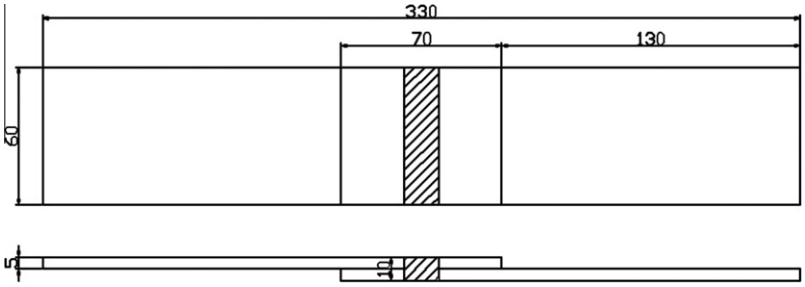

Fig. 2. Shape and size of the fatigue specimens (unit: mm).

EST is approximately the 84.3% of the top sheet thickness for the SPW joint and the 75.8% for the DPW joint respectively, therefore the DPW processes does not reduce the severe degree of hooking defects but increase that of hooking defects (Fig. 3a and b). It has been shown that the higher fatigue strength was achieved at the larger EST in aluminum alloys [20]. So the thinner of top sheet thickness for lap-welded joints caused by the hooking defect should decrease fatigue performance.

It is observed that hooking defects appeared at both AS and RS of FSW lap-welded joints. For the SPW joint, the hooking curves on both sides of welds firstly moved upward and were extended into the top plate in TMAZ, then had a downward orientation close to NZ. So a significant notch was found near the interface of NZ/TMAZ on both sides of welds. The smoother notch could do some extent to improve the fatigue property of lap-welded joint than that of the sharper one [21]. The gaps of the hooking defects became smaller when extending into NZ (Fig. 3c and d). Especially the hooking curves on RS had a larger rising trend ($L1 > L2$) as shown in Fig. 3a. The larger the up-trend was, the less the EST was and the worse the fatigue prosperity was indicated. So the fatigue fracture was the result of notches and up-trends co-functioning. For the DPW joint, the hooking on both sides of NZ moved upward and extended into the top sheet with interface gaps became smaller when closing to NZ. A slightly pull-down could be found only at RS. The hooking on AS had a slightly larger rising trend ($L3 > L4$) as shown in Fig. 3b and the hooking tip was acute where no notch was found, which made the fatigue property worse. The hooking defect is an adverse interface reorientation. It causes sharp discontinuities along the interface and creates acute tip where the stress becomes highly concentrated [10,21]. The fatigue fracture of FSW lap-welded joints always initiates at these places.

It can be seen from Fig. 3c and f that some faint and dark zigzag-lines that could be called the zigzag-line or kissing-bond defects appeared in the neighbor of stirring lap-interface zone. Oosterkamp et al. [22] suggested that the formation mechanism of the kissing-bond defect was related to the insufficient break-up of the oxide layer of initial joining surfaces by the insufficient stretch of the contacting surfaces around the tool pin. The increasing in heat input by high degree of the stirring could lead to the wider and diluter distribution of the oxide particles. Therefore the polishing pretreatment of initial lap interfaces should be necessary to remove these defects, and the optimization of the FSW process could prevent formation of the zigzag-line defect. It was found that the zigzag-line defect extended throughout the entire width of stirring lap-interface zone for the SPW joints (Fig. 3a, c and d). However, the zigzag-line defect is not obviously distinguishable in the DPW joint (Fig. 3b), and only a small part could be found near the NZ/TMAZ interface (Fig. 3f). This indicates that the DPW process could better mix material in the stirring lap-interface zone and is benefit to reduce the degree of zigzag-line defect. Due to the severest stress concentration is always existed at the tip of hooking defects, the experiment results shows that the fatigue crack growth was hardly along the zigzag-line defect during the whole fracture process, thus the fatigue properties were scarcely influenced by the existence of the zigzag-line defects.

As shown in Fig. 4a, the elongated grains are found in BM along the rolling direction. Meanwhile randomly-distributed and small Mg_2Si particles are also observed [23]. The HAZ undergoes a thermal cycle (Fig. 4b), but does not produces any plastic deformation, where grain structure and precipitates are getting coarsening. The microstructure of NZ is characterized by fine grains which belonged to the typical dynamic recrystallized organization. This structure was formed because of the high temperature and the fierce plastic deformation [24]. The grain size of the weld nugget at upper plate is bigger than that at lower plate (Fig. 4c and d), and this corresponds roughly to the temperature variation within the weld zone [25–27]. The bottom of lap-welded joint is contacted with the backing plate instead of the shoulder of tool, the peak temperature and thermal cycle are lower and shorter respectively as compared with that of top, which prevents the grain growth and results in smaller grains.

The typical micrographs of TMAZ are shown in Fig. 4e and f. The TMAZ undergoes both higher temperature and deformation during FSW, which is characterized by the obviously deformed structure.

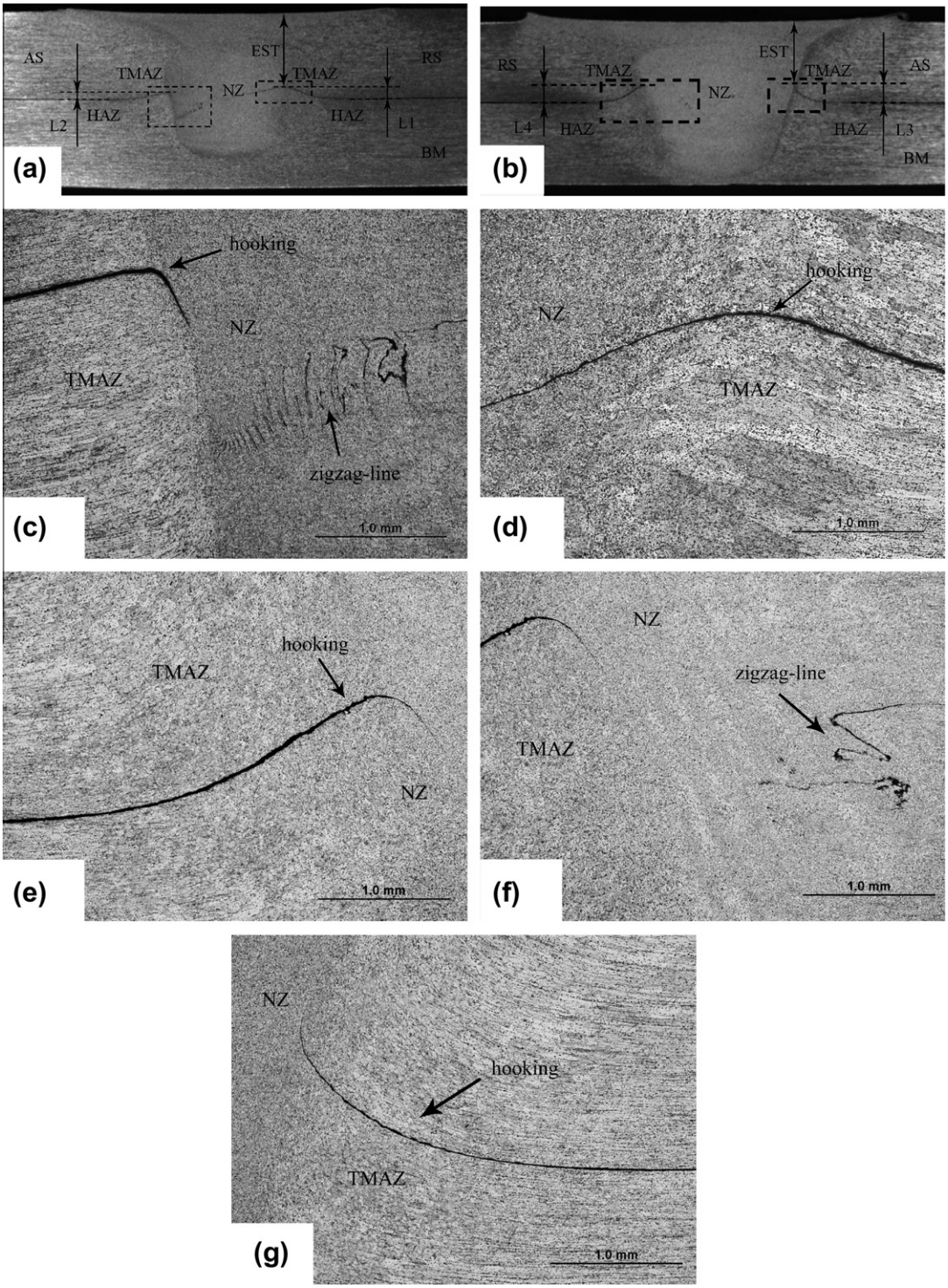

Fig. 3. Transverse cross section of the weld zone with various welding conditions: (a) the SPW overlap joint, (b) the DPW overlap joint. (c) A further magnified image of the left dashed box in (a), (d) a further magnified image of the right dashed box in (a), (e and f) a further magnified image of the left dashed box in (b), and (g) a further magnified image of the right dashed box in (b).

The elongated grains of base metal are deformed as an upward flowing mode around NZ. Because of the insufficient deformation strain, the recrystallization does not occur in this zone after TMAZ undergoing plastic deformation. The interface between NZ and TMAZ at AS is more distinctly visible than that at RS. The reason for this is that the plastic deforming directions of the weld metal and the base metal are opposite at AS and are consistent at RS. So there is a very big relative deformation between the base metal and the weld metal at AS, and the base metal distorted smoothly together with the welded metal at RS.

3.2. Fatigue properties

The statistical analysis of fatigue testing data in accordance with the IIW recommendations is performed and the *S–N* curves are plotted as shown in Fig. 5, which are expressed as the stress

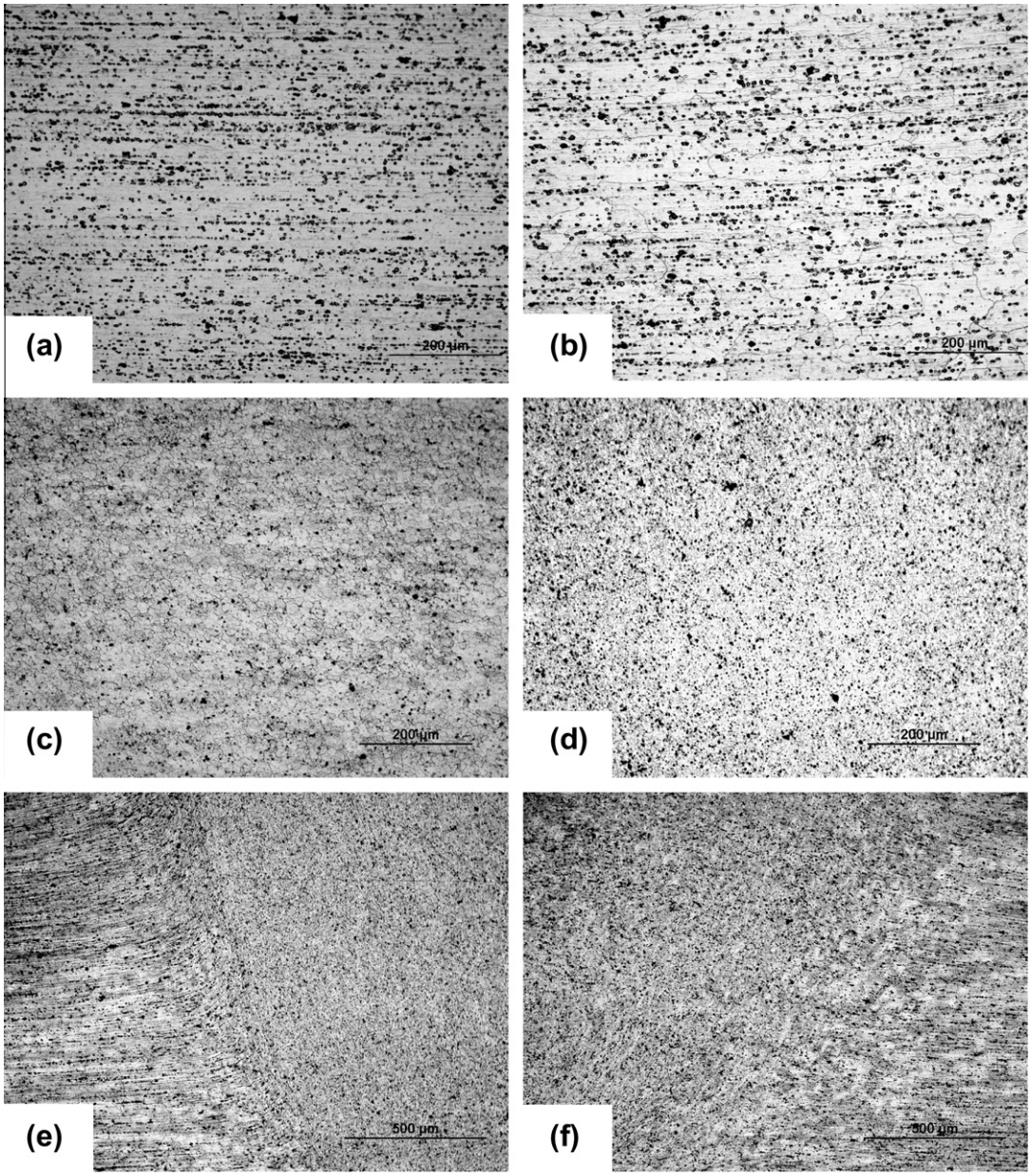

Fig. 4. Microstructures of FSW joints for AA6061: (a) BM, (b) HAZ, (c) NZ-up, (d) NZ-down, (e) TMAZ at AS, and (f) TMAZ at RS.

range $\Delta\sigma$ (MPa) versus the corresponding life to failure N (i.e. the number of cycles). The calculated characteristic values are listed in Table 2, in which the slope of S–N curve m, C_m and C_k are material constant. The IIW design curves of fusion lap-welded joint FAT22 (fatigue initiated by the toe crack) and FAT12 (fatigue initiated by the root crack) [16] are also plotted in the same figure for comparisons, and the fatigue testing statistical results for both fusion welded and FSW joints are listed in Table 3. According to IIW statistical method, the FSW testing results are calculated to determine the characteristic values of fatigue strengths $\Delta\sigma_m$ and $\Delta\sigma_k$ (corresponding to the 50% and 95% survival probability, respectively) associated to a two sided confidence interval of 75% of the mean C_m and of the standard deviation S.D. of β = 75% (12.5% probability of being above or below the extreme value of the confidence interval) at 2×10^6 cycles.

It can be seen that all of the FSW testing points are obviously lower than that of IIW FAT22 (toe crack), and roughly correspond and close to the IIW FAT12 design curve (root crack). The slope values of FSW S–N curves are very different from that of IIW S–N curves (Fig. 5 and Table 2). The IIW recommendations of fusion welded joints are m = 3.0–3.5 which was lower than that m = 6.0–8.0 of FSW lap-welded joints. The fatigue strengths $\Delta\sigma_k$ (with 95% survival probability) of FAT12 (root crack) for fusion lap-welded joints are 13.92 MPa (R = 0.1), 12.96 MPa (R = 0.3) and 12 MPa (R = 0.5) respectively. For FSW lap-welded joints, the value $\Delta\sigma_k$ of fatigue strengths are between 10.65 MPa and 15.27 MPa. Although the fatigue strengths of FSW joints are higher than that of FAT12 in the lower stress range ($N > 10^6$), the values of FSW are really lower than that of FAT12 in the higher stress range ($N < 10^6$). The fatigue properties of FSW lap-welded joints are not always excelled to that of fusion lap-welded joints and only approximately correspond to the fatigue strength of FAT12 (root crack).

It also indicates that all of the FSW testing results are located below the characteristic S–N curve of SPW joint with R = 0.1. For the same joints (SPW or DPW), the increase of R will lead to the decrease of fatigue strength under the same cycle life N. The

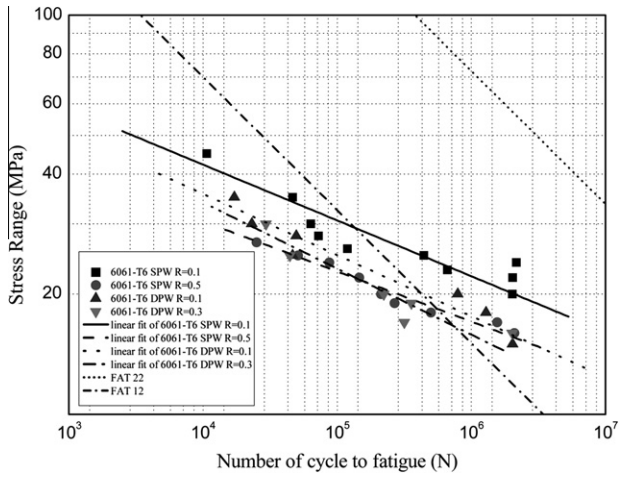

Fig. 5. *S–N* curves under different conditions.

Table 2
The calculated results of the fatigue data of AA6061 overlap joints.

Type	R	m	C_m	$\Delta\sigma_m$ (MPa)	C_k	$\Delta\sigma_k$ (MPa)
SPW	0.1	7.15	4.27×10^{15}	20.13	5.90×10^{14}	15.27
SPW	0.5	7.96	6.52×10^{15}	15.65	2.89×10^{15}	14.13
DPW	0.1	6.53	1.37×10^{14}	15.85	2.96×10^{13}	12.54
DPW	0.3	6.04	1.76×10^{13}	14.12	3.21×10^{12}	10.65

Table 3
Comparison of fatigue strength between FSW joints and IIW specification.

Structural detail	Description	R	Category	FAT (MPa)
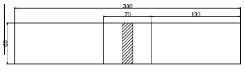	Transverse loaded overlap joint with friction stir welds	0.1	1	15.27
			2	12.54
	1:SPW	0.3	2	10.65
	2:DPW	0.5	1	14.13
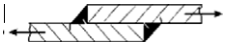	Transverse loaded overlap joint with fillet welds	0.1	1	25.52
			2	13.92
	1:Stress in plate at weld toe (toe crack)	0.3	1	23.76
			2	12.96
	2:Stress in weld throat (root crack)	0.5	1	22
			2	12

fatigue strength $\Delta\sigma_m$ of SPW joint is decreasing from 20.13 MPa to 15.65 MPa when $R = 0.1$ is changing into $R = 0.5$, and the $\Delta\sigma_m$ of DPW joint is reducing from 15.85 MPa to 14.12 MPa when $R = 0.1$ changing into $R = 0.3$. In addition it is shown that the difference of slope values for the two *S–N* curves of SPW and DPW joints are small (*D*-values were 0.81 for SPW joints and 0.49 for DPW joints respectively). The two characteristic fatigue curves appeared approximately parallel (for double-logarithm coordinates) in the whole region between 2×10^3 cycles and 2×10^7, which meant that the influence of R on fatigue life was limited.

For the given fatigue stress ratio R (Table 2), the calculated results indicate that the fatigue strength $\Delta\sigma_m$ ($R = 0.1$) decreases from 20.13 MPa for the SPW joint to 15.85 MPa for the DPW joint representing a reduction of 21.26% in fatigue performance. Furthermore the characteristic fatigue strength $\Delta\sigma_k$ ($R = 0.1$) also decreases from 15.27 MPa for the SPW joint to 12.54 MPa for the DPW joint with a reduction of 17.88%. The *S–N* curve of DPW joints is steeper with a slope of $m = 6.53$ than that of SPW joints with a slope of $m = 7.15$. Because of this varying tendency the difference between the two curves will gradually become bigger in the cycle life of $N \geqslant 2 \times 10^6$ ranges. These facts indicate that the fatigue properties of SPW joints are superior to that of DPW joints. However, the difference of the two *S–N* curves is becoming relatively smaller in the high stress range/low fatigue life regime.

3.3. Fractography

Fatigue testing results shows that all the SPW specimens fractured at RS and all the DPW specimens fractured at AS (Fig. 6a and b). These fracture locations correspond to more serious hooking defect, of which the up-trend was larger. The upper plate thinning phenomenon is clearly observed. As mentioned above, the up-trend of the hooking defect is an important factor of fatigue strength. There are different levels of necking phenomenon at the fracture place. In the cracked weld, the fatigue fracture is initiated from the tip of the hooking defect lines due to the presence of severe stress concentration and propagates into the NZ (Fig. 6c and d). All the specimens were fractured in the weld region and have more tidy edges.

Fig. 7 shows some typical fatigue fracture surface of SPW joints. The fatigue fractography consists of several different zones, which include fatigue crack initiation, propagation and the final fracture zone. It can be seen that the fracture exhibits multiple crack initiations from the bottom of the upper plate corresponding to the hooking location as shown in Fig. 7a. With the distance from the bottom surface increasing, the fracture surface could be divided into two parts: propagation area is much smoother with some fatigue strips on the surface; the final fracture area is relatively coarser with an obvious plastic deformation and tearing ridge features. Meanwhile some apparent oval traces are clearly found. The propagation shows some brittle fracture features and some secondary cracks are found (Fig. 7b). Fatigue striations are clearly observed at higher magnifications (Fig. 7c), of which the light horizontal lines marked the advance of a crack through the part with each cycle. As shown in Fig. 7d, the ductile cracking associated with many deep-hole type dimples are found in the final fracture zone. It is obviously observed that the different shapes and sizes of second phase coarse particles located in the dimples.

Fig. 8 shows some typical fatigue fracture surface of DPW joints. It can be seen that the fracture also exhibits multiple crack initiations from the bottom of the upper plate corresponding to the hooking location as shown in Fig. 8a, but the locations of crack initiation are more than that of SPW joints, which is one reason of the poor fatigue property. Especially the intergranular cracking along the weak grain boundaries (Fig. 8b and c) demonstrated the initiation sites were located in the NZ and shows crystallographic fracture mode. The crack propagation is also mainly characterized by the characteristic fatigue striations (Fig. 8d and e), but this area has more secondary cracks getting the fatigue property worse. Shallow-hole type dimples were observed on the final fracture area (Fig. 8f). No second phase coarse particles could be found.

4. Conclusions

(1) The fatigue strength of FSW lap-welded joints for AA6061-T6 alloys are obviously lower than that of the fusion lap-welded joints of IIW FAT22 (fatigue initiated by the toe crack), and only approximately correspond and close to the IIW FAT12 design curve (fatigue initiated by the root crack). The slope values $m = 6.0–8.0$ of FSW *S–N* curves are very different from that $m = 3.0–3.5$ of IIW *S–N* curves and the fatigue strength of FSW lap-welded joints always lower than

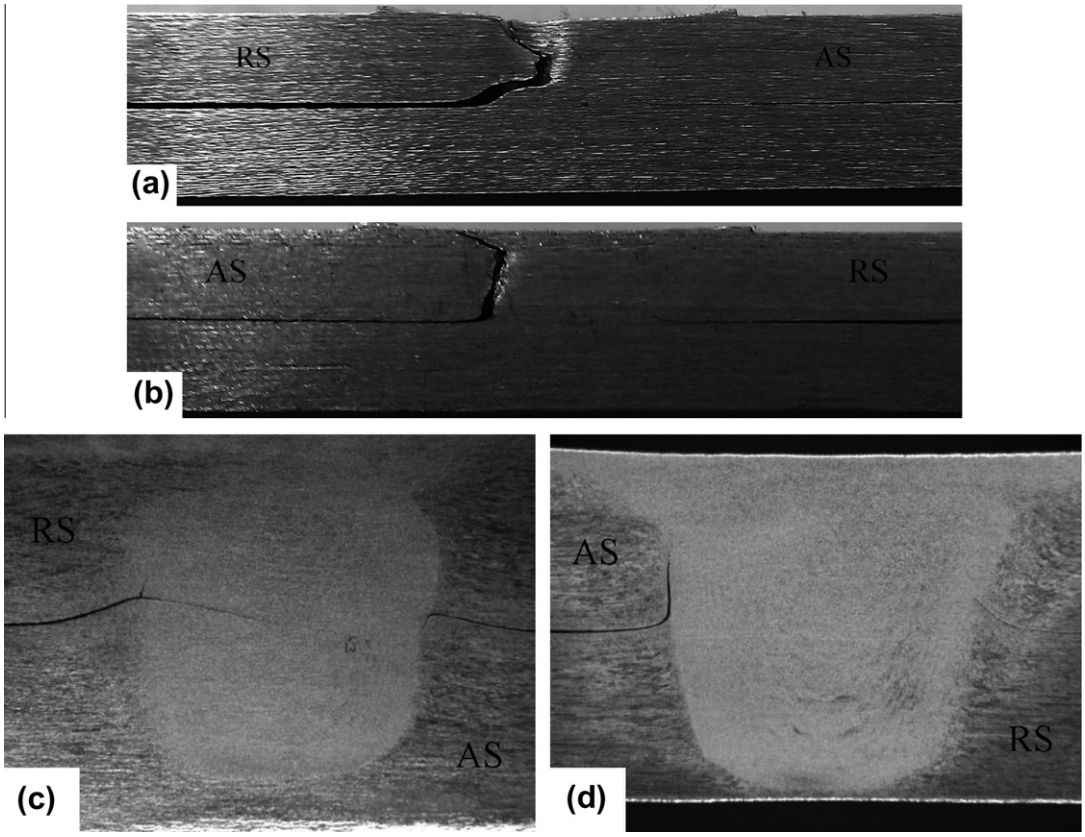

Fig. 6. Typical failure locations of the two joints: (a) appearance of a failed SPW fatigue specimen, (b) appearance of a failed DPW specimen, (c) transverse cross section of another failed SPW fatigue specimen after being etched and (d) transverse cross section of another failed DPW fatigue specimen after being etched.

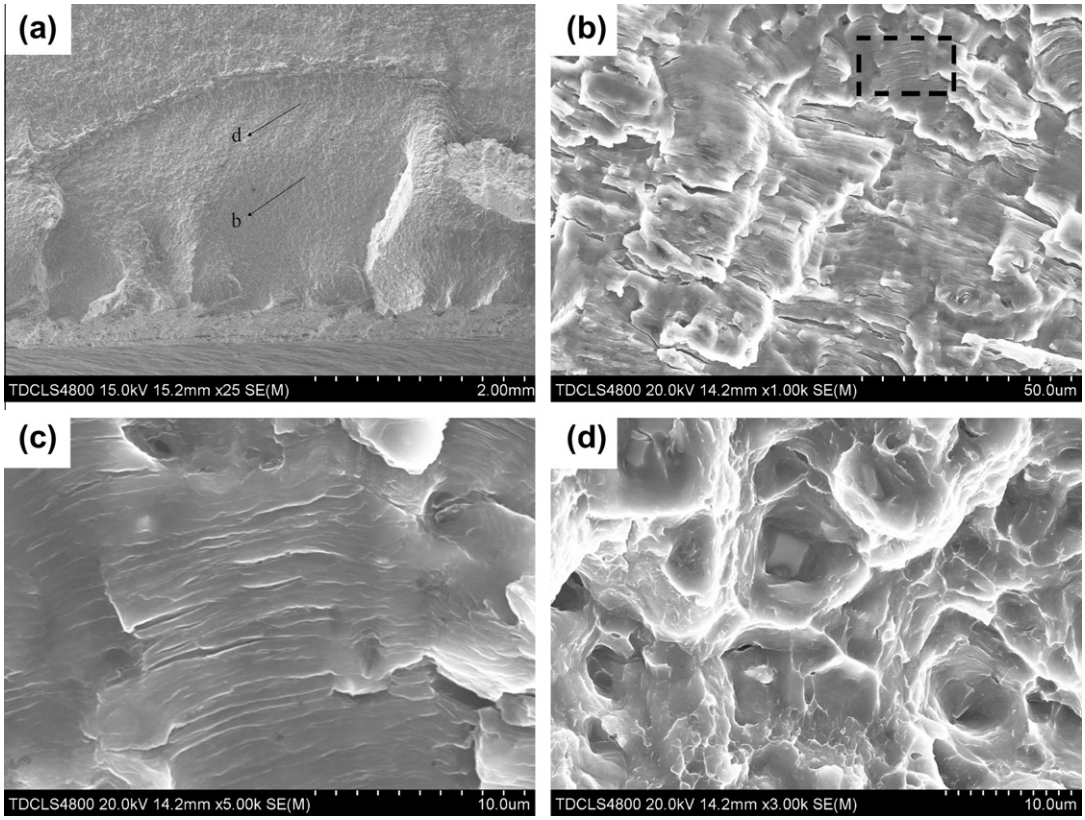

Fig. 7. SEM images of fatigue fracture surfaces of the SPW specimen tested at 17 Mpa stress amplitude ($R = 0.5$): (a) overall view of the fracture surface at a lower magnification, (b) the fatigue crack propagation zone, (c) fatigue striations at a higher magnification of the dashed box in (b), (d) the final fracture region.

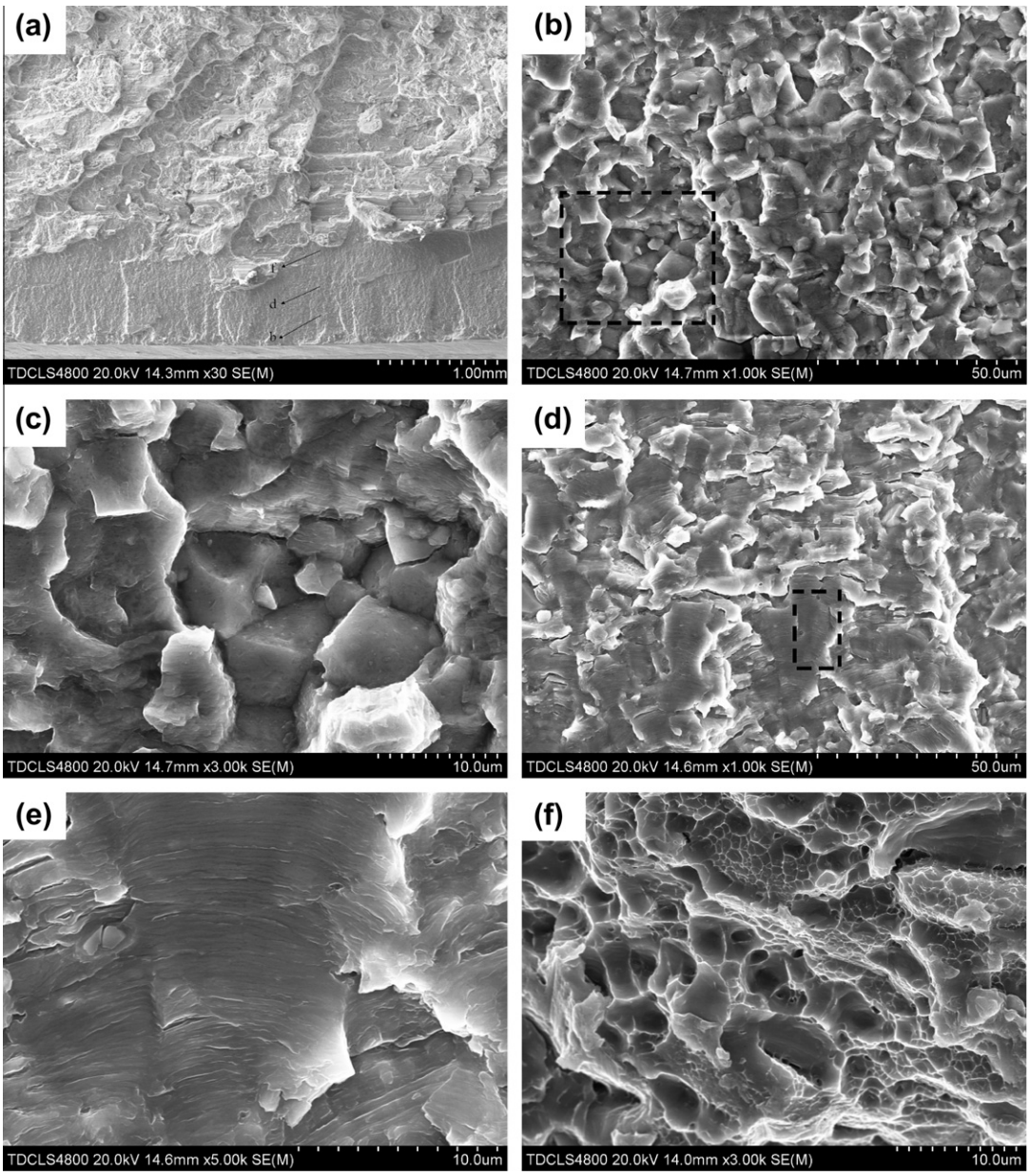

Fig. 8. SEM images of fatigue fracture surfaces of the DPW specimen tested at 30 Mpa stress amplitude ($R = 0.3$): (a) overall view of the fracture surface at a lower magnification, (b) magnified view near initiation, (c) intergranular cracking along the weak grain boundaries of equiaxed grains, (d) the fatigue crack propagation zone, (e) fatigue striations at a higher magnification of the dashed box in (d), (f) the final fracture region.

that of fusion lap-welded joints in the higher stress/shorter life range ($N < 10^6$ cycles). The higher fatigue stress ratio R will lead to the decrease of fatigue strength of FSW lap-welded joints.

(2) The existence of hooking defects in FSW lap-welded joints is the key factor to reduce the fatigue strengths. The hooking defects are one of the interface reorientation defects located in the TMAZ of FSW lap-welded joints, which can obviously decrease the effective sheet thickness of lap-welded joints and produce severe stress concentrations. Fatigue cracks always initiate at the tip of hooking defect in the RS of SPW and AS of DPW joints respectively, and then propagate into the NZ leading to the final fracture of fatigue specimens.

(3) The faint and dark zigzag-line defects can be formed in the neighbor of lap-interface zone for FSW lap-welded joints, which are produced by the residual oxide layer of initial lap-joining surfaces. The DPW process could effectively mix the material of lap-interface zone and reduce the degree of zigzag-line defects as compared with the SPW process. But the fatigue properties of FSW lap-welded joints are scarcely influenced by the existence of the zigzag-line defects.

(4) The severity of hooking defects and the quality of lap-welds could not be improved by the DPW process as compared with the SPW process. In contrary the DPW process will produce the more serious hooking defects, lead to the decrease of effective sheet thickness and final reduce the fatigue strength of FSW lap-welded joints. The fatigue strength $\Delta\sigma_m$ and $\Delta\sigma_k$ ($R = 0.1$) of DPW joints will be 21.26% and 17.88% lower than that of SPW joints respectively. So the fatigue properties of SPW joints are superior to that of DPW joints.

(5) The fatigue fractography consists of several different zones, which includes the fatigue crack initiation, propagation and the final fracture zone. The fracture surfaces of FSW lap-welded joints exhibited multiple crack initiations from

the bottom of the upper plate corresponding to the hooking locations. The crack propagation shows some brittle fracture features and is mainly characterized by the characteristic fatigue striations. The intergranular cracking along the weak grain boundaries found in the DPW specimen demonstrates the initiation sites are located in the NZ and shows crystallographic fracture mode. The locations of crack initiation and the amount of secondary cracks are more in the DPW specimen than that in the SPW specimen which getting the fatigue property worse. Ductile fracture modes are obviously shown in the final fracture zone with deep-hole type dimples in the SPW specimen but shallow-hole type dimples in the DPW specimen.

Acknowledgement

The authors wish to thank the National Nature Science Foundation of China for the financial support for this research project (No. 50775159).

References

[1] Thomas WM, Nicholas ED, Needham JC, Church MG, Templesmith P, Dawes CJ. Friction stir welding. International patent application no. PCT/GB92102203 and Great Britain patent application no. 9125978.8; 1991.
[2] Bussu G, Irving PE. The role of residual stress and heat affected zone properties on fatigue crack propagation in friction stir welded 2024-T351 aluminum joints. Int J Fatigue 2003;25:77–88.
[3] Thomas WM, Nicholas ED. Friction stir welding for the transportation industries. Mater Des 1997;18:269–73.
[4] Sato YS, Kokawa H, Enomoto M, Jogan S. Microstructural evolution of 6063 aluminum during friction stir welding. Metall Mater Trans A 1999;30:2429–37.
[5] Feng AH, Chen DL, Ma ZY. Microstructure and low-cycle fatigue of a friction-stir-welded 6061 aluminum alloy. Metall Mater Trans A 2010;41A:2626–41.
[6] Mishra RS, Ma ZY. Friction stir welding and processing. Mater Sci Eng R 2005;50:1–78.
[7] Xu WF, Liu JH, Luan GH, Dong CL. Microstructure and mechanical properties of friction stir welded joints in 2219-T6 aluminum alloy. Mater Des 2009;30:3460–7.
[8] Christner B, Mc Coury J, Higgins S. Development and testing of friction stir welding as a joining method for primary aircraft structure. In: 4th international symposium on friction stir welding, Park city, UT, USA, session 4A, May 14–16. Cambridge CB1 6AL, UK: TWI Ltd., Abington; 2003.
[9] Buffa G, Campanile G, Fratini L, Prisco A. Friction stir welding of overlap joints: influence of process parameters on the metallurgical and mechanical properties. Mater Sci Eng A 2009;519:19–26.
[10] Ericsson M, Jin LZ, SandstrÖm R. Fatigue properties of friction stir overlap welds. Int J Fatigue 2007;29:57–68.
[11] Christner B, McCoury J, Higgins S. Development and testing of friction stir welding (FSW) as a joining method for primary aircraftstructure. In: Proceedings of the 4th international symposium on FSW, Park city; 2003.
[12] Cederqvist L, Reynolds AP. Properties of friction stir welded aluminium overlap joints. In: Proceedings of the 2nd international symposium on FSW, Gothenburg; 2000.
[13] Ericsonn M, Sandstrom R. Fatigue of FSW overlap joints in aluminium welded with different tool designs. In: Fifth international symposium on friction stir welding, Metz, France; September 14–16, 2004.
[14] Fersini D, Pirondi A. Analysis and modelling of fatigue failure of friction stir welded aluminum alloy single-overlap joints. Eng Fract Mech 2008;75:790–803.
[15] Colegrove PA, Shercliff HR, Thyoe. Development of the trivex™ friction stir welding tool for making overlap welds. In: Fifth international symposium on friction stir welding. Metz, France; September 14–16, 2004.
[16] IIW joint working group XIII–XV, Chairman A. Hobbacher. IIW fatigue recommendations, IIW document XIII-1539-96/XV-845-96, update March 2002.
[17] Japanese industrial standard (JIS). JIS Z 3138-1989: Method of fatigue testing for spot welded joint. Released on 1989 March 1.
[18] Khodir SA, Shibayanagi T. Friction stir welding of dissimilar AA2024 and AA7075 aluminum alloys. Mat Sci Eng B 2008;148:82–7.
[19] Cao X, Jahazi M. Effect of tool rotational speed and probe length on overlap joint quality of a friction stir welded magnesium alloy. Mater Des 2011;32:1–11.
[20] Cederqvist L, Reynolds AP. Factors affected the properties of friction stir welded aluminum overlap joints. Weld J (Res Suppl) 2001:281–7.
[21] Cantin GM, David SA, Lara-Curzio E, Babu SS. Microstructure characteristics and mechanical properties of friction skew-stir welded lap joints in 5083-O aluminum. In: Proceedings of the 7th international conference on trends in welding research, Callaway gardens resort, Pine mountains, Georgia, USA; May 16–20, 2005. p. 185–90.
[22] Oosterkamp A, Oosterkamp LD, Nordeide A. 'Kissing bond' phenomena in solid-state welds of aluminum alloys. Weld J 2004;83:225s–31s.
[23] Madhusudhan Reddy G, Mastanaiah P, Sata Prasad K, Mohandas T. Microstructure and mechanical property correlations in AA 6061 aluminium alloy friction stir welds. Trans Indian Inst Met 2009;62:49–58.
[24] Jata KV, Semiatin SL. Continuous dynamic recrystallization during friction stir welding of high strength aluminium alloys. Scr Mater 2000;43:743–9.
[25] Murr LE, Li Y, Flores RD, Trillo EA, McClure JC. Intercalation vortices and related microstructural features in the friction-stir welding of dissimilar metals. Mater Res Innovations 1998;2:150–63.
[26] Li Y, Murr LE, McClure JC. Flow visualization and residual microstructures associated with the friction-stir welding of 2024 aluminum to 6061 aluminum. Mater Sci Eng A 1999;271:213–23.
[27] Murr LE, Liu G, McClure JC. Dynamic recrystallization in friction-stir welding of aluminium alloy 1100. J Mater Sci Lett 1997;16:1801–3.